



OPEN ACCESS

EDITED BY

Hong-Hu Zhu,
Nanjing University, China

REVIEWED BY

Dongsheng Xu,
Wuhan University of Technology, China
Gang Cheng,
North China Institute of Science and
Technology, China

*CORRESPONDENCE

Wenbo Zheng,
✉ 2021026038@chd.edu.cn

RECEIVED 25 November 2024

ACCEPTED 27 January 2025

PUBLISHED 05 March 2025

CITATION

Jing P, Zheng W, Wang H, Wang Y and Yang H
(2025) Investigation on the influence of
structural surface characteristics on stress
wave propagation behavior.
Front. Earth Sci. 13:1534007.
doi: 10.3389/feart.2025.1534007

COPYRIGHT

© 2025 Jing, Zheng, Wang, Wang and Yang.
This is an open-access article distributed
under the terms of the [Creative Commons
Attribution License \(CC BY\)](https://creativecommons.org/licenses/by/4.0/). The use,
distribution or reproduction in other forums is
permitted, provided the original author(s) and
the copyright owner(s) are credited and that
the original publication in this journal is cited,
in accordance with accepted academic
practice. No use, distribution or reproduction
is permitted which does not comply with
these terms.

Investigation on the influence of structural surface characteristics on stress wave propagation behavior

Pengxu Jing^{1,2}, Wenbo Zheng^{1*}, Haiying Wang², Yang Wang²
and Haitao Yang³

¹College of Geology Engineering and Geomatics, Chang'an University, Xi'an, Shaanxi, China, ²Key Laboratory of Life Search and Rescue Technology for Earthquake and Geological Disaster, Ministry of Emergency Management, Beijing, China, ³College of Earth Science and Engineering, Shandong University of Science and Technology, Qingdao, China

When stress waves propagate in rock slopes, they are influenced by various factors such as structural plane characteristics (e.g., stiffness, number, spacing, thickness), sawtooth structural characteristics (e.g., stiffness, angle of sawtooth structural planes), filling materials (fully filled, partially filled, and different filling materials), and wave impedance properties, leading to phenomena such as amplitude attenuation, signal delay, and wave velocity reduction. In this paper, using the one-dimensional Hopkinson bar model as an example, a numerical method is employed to analyze the propagation behavior of stress waves through structural planes with different characteristics. By monitoring key parameters such as permanent displacement, acceleration, and stress values of the stress waves, the influencing laws are revealed: When the stiffness of the structural planes exceeds a certain critical threshold (i.e., 2.8×10^6 Pa), the permanent displacement, acceleration, and stress values of the stress waves significantly increase with increasing stiffness. The increase in structural plane spacing promotes significant growth in the permanent displacement, acceleration, and stress values of the stress waves, which is another key factor affecting the propagation characteristics of stress waves. Conversely, as the number and thickness of structural planes increase, the response parameters of the stress waves exhibit a decreasing trend, revealing the hindering effect of dense and thickened structural planes on stress wave propagation. An increase in the angle of sawtooth structural planes exacerbates the reflection and attenuation of stress waves, leading to a significant reduction in the peak values of permanent displacement and acceleration, which further emphasizes the influence of structural plane morphology on the propagation path and energy distribution of stress waves. Additionally, the density of filling materials has proven to be a non-negligible factor, as its increase helps reduce energy dissipation, thereby enhancing the propagation effect of stress waves. In cases where there is a significant difference in wave impedance, the amplitude and propagation velocity of stress waves are significantly reduced, highlighting the importance of wave impedance matching in wave propagation. Furthermore, an increase in the damping ratio further accelerates the energy dissipation process, resulting in a significant reduction in the amplitude of stress waves at the propagation endpoint, which emphasizes the crucial role of damping effects in the attenuation of stress wave energy. The research results provide a theoretical basis for the analysis of rock mass dynamic behavior and rock slope stability,

and have important guiding significance for the engineering design and disaster prevention of geomaterials under complex geological conditions.

KEYWORDS

stress wave propagation, structural plane characteristics, filling material, wave impedance, damping ratio, rock mass dynamics

1 Introduction

In recent years, the study of structural planes, their characteristics, and the propagation patterns of stress waves has garnered widespread attention. This is primarily due to their decisive role in the stability of rock masses, thereby exerting a profound influence on engineering construction (Chai et al., 2020; Huang J. et al., 2020; Jia et al., 2021). Characteristics of structural planes, wave impedance, damping, and other factors can lead to phenomena such as attenuation of stress wave amplitudes, signal delay, and wave speed reduction (Müller et al., 2010; Song, 2012; Shafique et al., 2020; Zhou et al., 2021). Therefore, it is essential to conduct in-depth research on the characteristics of structural planes and their parameter variations, exploring the propagation patterns of stress waves passing through structural planes.

In practical engineering applications, exploring the propagation patterns of stress waves in structural planes has practical value. In mining engineering, studying the propagation patterns of stress waves through soft rocks is crucial for improving mining efficiency and ensuring the safety of tunnels (Qin et al., 2023; Wang et al., 2023). In geotechnical engineering, the stability of rocky slopes is frequently governed by multiple structural planes with varying attitudes (Wei et al., 2024; Zheng et al., 2024). Slope stability is significantly influenced by the attenuation and propagation behavior of stress waves through primary structural planes (Song et al., 2021). A systematic study of stress wave propagation in diverse structural planes is essential to understanding potential failure modes of rocky slopes and ensuring engineering safety. In earthquake engineering, thoroughly investigating the interaction between stress waves and structural planes has indispensable guiding significance for the design of key components such as anchor rods and anchor cables. It is also a critical aspect of ensuring earthquake resistance and fortification effects (Wang et al., 2022; Yu et al., 2024). By accurately grasping the propagation characteristics of stress waves in different structural planes, we can more effectively carry out earthquake-resistant design and disaster prevention, thereby protecting the safety of people's lives and property.

In recent years, significant progress has been made in studying the influence of structural surface characteristics on the propagation of stress waves. Scholars have thoroughly investigated the effects of different structural surface characteristics (such as linear structural surfaces, nonlinear structural surfaces, filled structural surfaces, etc.) on the propagation of stress waves through various means, including theoretical derivation, numerical simulation, and experimental verification (Zeng et al., 2018; Feng et al., 2020; Li et al., 2021; Lou et al., 2021). In terms of theoretical derivation, research on stress wave propagation in jointed rock masses primarily focuses on two approaches: displacement discontinuity theory and equivalent medium theory (Chong et al., 2020; Zhu et al., 2020; Fan et al., 2021). Displacement discontinuity theory assumes that

joint surfaces consist of a colinear plane made up of voids and contact points. The theory posits that displacement is discontinuous at the joint, while stress remains continuous, making it suitable for studying phenomena like joint crack opening, closing, and slipping (Zheng et al., 2021; Xiroudakis et al., 2023; Zhang et al., 2024; Nolte et al., 2000). Evaluated the applicability of displacement discontinuity theory, concluding that it becomes invalid when joint thickness approaches the incident wave's wavelength or when severe distortion arises at joint contact points, causing resonant scattering. Equivalent medium theory models rocks and structural planes, such as joints and fractures, as a continuous medium, using equivalent elastic modulus to describe stress wave attenuation in rock masses. This approach is primarily used to analyze stress wave propagation and attenuation in highly jointed rock masses (Liu et al., 2000; Huang X. et al., 2020; Kim et al., 2021; White, 2000) applied equivalent medium theory to study stress wave propagation in rocks with parallel joints, deriving the relationship between equivalent elastic modulus, joint stiffness, and spacing, and formulated the stress wave velocity attenuation equation (Yu et al., 2012). Utilized nonlinear wave theory and the BB model of structural planes to examine how dual nonlinearity in rock masses and structural planes affects stress wave propagation (Li et al., 2012). Developed a time-domain recursive method to investigate the transmission and reflection of P-waves and S_V -waves incident at an angle to parallel linear and nonlinear structural planes (Fan et al., 2012). introduced a nonlinear viscoelastic equivalent medium model to analyze P-wave propagation in rock masses with parallel structural planes under vertical incidence. In terms of numerical simulation, with the ongoing development of computer technology, numerical simulation has gradually become an important means to study the propagation of stress waves in rock masses with complex structural surfaces. Numerical simulation software, such as UDEC and LS-DYNA, is widely used to simulate the propagation of stress waves in rock masses with structural surfaces of different dip angles, fillings, and various stiffness values. This reveals the influence of structural surface characteristics on the propagation path, energy attenuation, and dynamic response of stress waves (Chai et al., 2020; Fan and Cai, 2021; Rong et al., 2024). In terms of experimental verification, scholars have collected stress wave propagation data through methods such as SHPB tests and on-site blasting experiments, verifying the correctness of theoretical derivations and numerical simulation results. For example, the SHPB test has been used to study the influence of factors such as joint stiffness and incident wave frequency on the transmission and reflection coefficients of cylindrical waves in single-jointed rock masses (Hong et al., 2021; Li et al., 2021).

Despite significant progress, there are still some shortcomings in current research. First, regarding the simulation of complex structural surfaces: The morphology of structural surfaces in actual rock masses is complex and diverse, including different dip angles,

fillings, and various stiffness values, among others. However, most existing studies focus on single or simplified combinations of structural surface characteristics, making it difficult to fully capture the complexity of structural surfaces in actual rock masses (Xia et al., 2020; Guo et al., 2022). Second, considering multi-field coupling effects: The propagation of stress waves in rock masses is not only affected by the characteristics of structural surfaces but also by coupled factors such as ground stress and temperature. However, most existing studies have ignored these multi-field coupling effects, leading to certain limitations in the practical applications of research results (Liu et al., 2020; Chen et al., 2022). Third, regarding the limitations of experimental data: Experimental verification is an important aspect of theoretical research, but experimental data often have limitations due to experimental conditions (Zarastvand et al., 2022). For example, it is difficult to precisely control experimental conditions in *in-situ* blasting experiments, resulting in fluctuations and uncertainties in the data. Finally, concerning the applicability of theoretical models: Theoretical derivations are often based on certain assumptions and simplified conditions, thus limiting the extent to which these models can be applied in practice (Wang et al., 2018; Kononenko and Khomeenko, 2021). For example, although the equivalent medium method can simplify the calculation process, it is difficult to accurately reflect the complexity of structural surfaces in actual rock masses (Aligholi and Khandelwal, 2022). In summary, future research should further focus on simulating the complexity of structural surfaces, analyzing multi-field coupling effects, accurately collecting experimental data, and verifying the applicability of theoretical models. This will provide a more comprehensive understanding of how structural surface characteristics influence the propagation of stress waves.

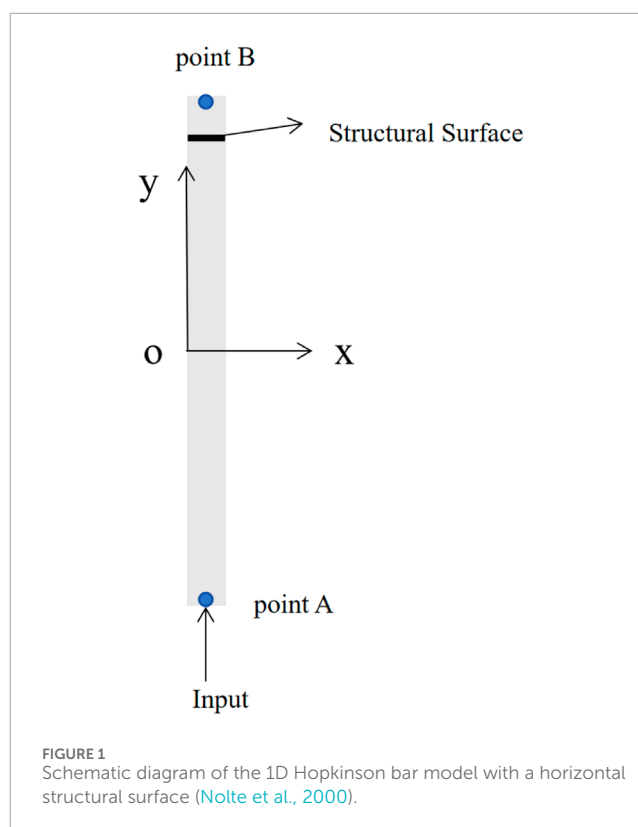
This paper uses a one-dimensional Hopkinson bar (100 m long and 1 m wide) to investigate the propagation behavior of stress waves through various structural planes. Figure 1 presents a schematic diagram of the structural plane model.

2 Influence of structural surface characteristics

The model in Figure 1 applies fixed constraints and viscoelastic boundary conditions to the bottom surface of the Hopkinson bar. A sinusoidal velocity pulse, with a frequency of 10 Hz and amplitude of 1 m/s, is introduced at point A. One or more structural planes are positioned along the midsection of the bar. At point B, the permanent displacement, stress, and acceleration of stress waves transmitted through the structural planes are recorded. The propagation behavior of stress waves is analyzed by varying the stiffness, number, spacing, and thickness of the structural planes, utilizing an improved Newmark model.

The one-dimensional Hopkinson bar is modeled as a two-dimensional rectangle with dimensions of 100 m × 1 m. Quadrilateral elements with dimensions of 0.5 m × 0.5 m are used for the mesh, as illustrated in Figure 2.

The material parameters of the model are shown in Table 1.



2.1 Structural surface stiffness

The effect of varying stiffness in horizontal structural planes on stress wave propagation is analyzed. Stiffness values of 2.8×10^4 Pa, 2.8×10^5 Pa, 2.8×10^6 Pa, 2.8×10^7 Pa and 2.8×10^8 Pa are analyzed.

By varying the stiffness of a single horizontal zero-thickness structural plane, vertical permanent displacement curves for different stiffness values were obtained, as shown in Figure 3. For structural plane stiffness values above 2.8×10^6 Pa, both vertical permanent displacement and its growth rate increase with rising stiffness. When stiffness is below 2.8×10^6 Pa, the changes in permanent displacement and its growth rate are negligible, consistent with observed results. At stiffness levels below 2.8×10^6 Pa, the system behaves like a one-dimensional Hopkinson bar without a structural plane, resulting in minimal change in permanent displacement.

As shown in Figure 4, the y-direction acceleration curves indicate that for structural plane stiffness values exceeding 2.8×10^6 Pa, the acceleration increases with higher stiffness. For stiffness values below 2.8×10^6 Pa, the acceleration curves show minimal change. Higher structural plane stiffness results in greater acceleration values at the endpoint and earlier stress wave propagation, consistent with observed data.

As shown the y-direction stress curves indicate that stress waves are detected earliest at a stiffness of 2.8×10^8 Pa, followed by 2.8×10^7 Pa. For stiffness values below 2.8×10^6 Pa, the stress wave values are minimal, aligning with observed results. Lower

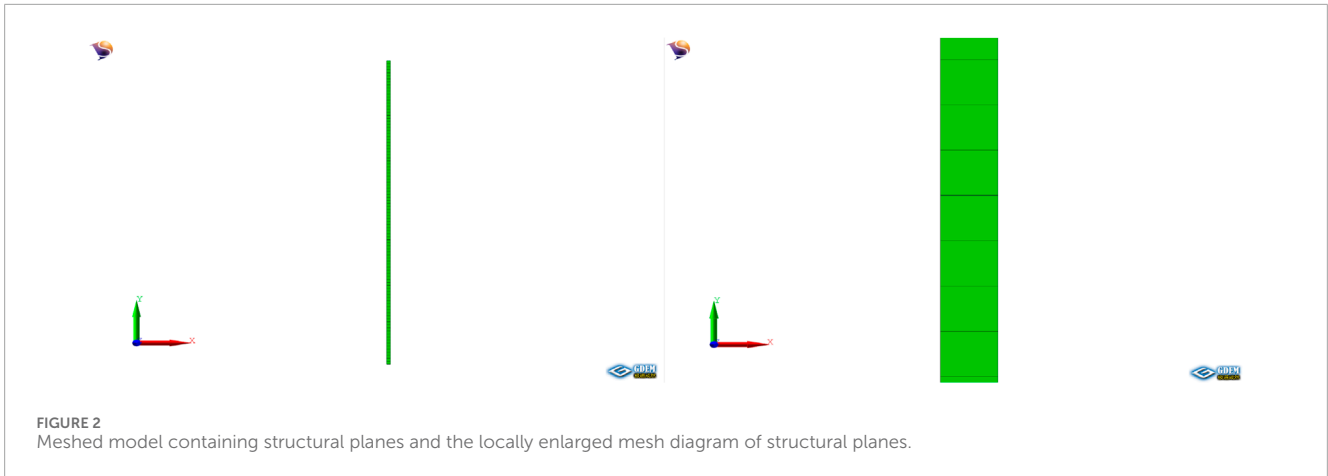


FIGURE 2 Meshed model containing structural planes and the locally enlarged mesh diagram of structural planes.

TABLE 1 Material parameters of the model.

Model parameters	Density (kg/m ³)	Elastic modulus (Pa)	Poisson's ratio	Cohesion (Pa)	Tensile strength (Pa)	Friction angle (°)
	2700	6.5628e10	0.2	4.0e5	2.0e5	35
Interface Parameters	Normal Stiffness (Pa)	Shear Stiffness (Pa)	Friction Angle (°)	Cohesion (Pa)	Tensile Strength (Pa)	Dilatancy Angle (°)
	2.8e8	2.8e8	15	1.0e5	1.0e4	8

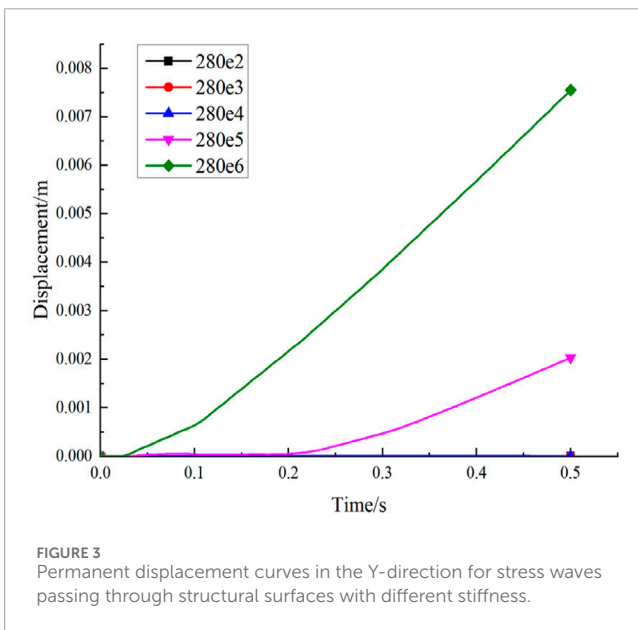


FIGURE 3 Permanent displacement curves in the Y-direction for stress waves passing through structural surfaces with different stiffness.

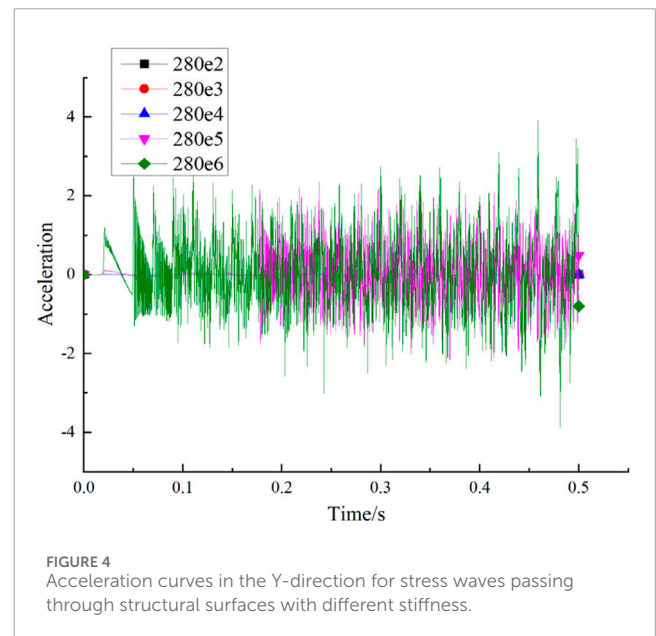
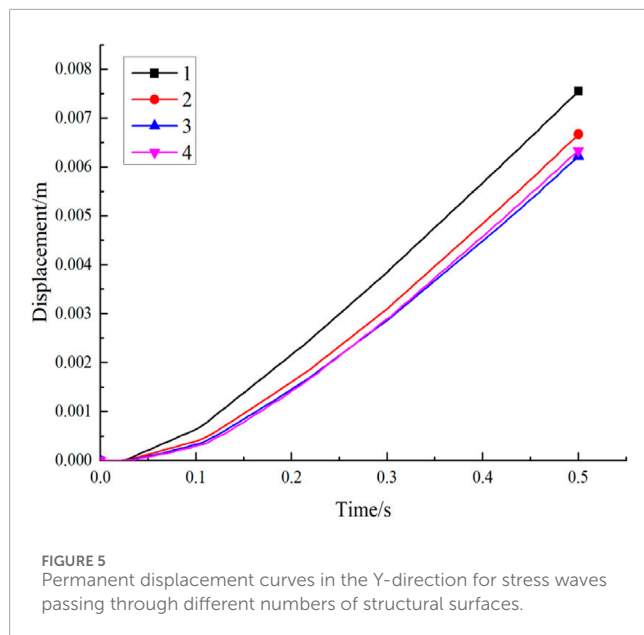


FIGURE 4 Acceleration curves in the Y-direction for stress waves passing through structural surfaces with different stiffness.

stiffness in structural planes induces significant refraction and reflection of stress waves, resulting in a gradual reduction in their propagation speed.

The above discussion reveals that when the structural plane stiffness exceeds 2.8×10^6 Pa, y-direction permanent displacement, acceleration, and stress values increase with higher stiffness. This highlights the role of high-stiffness structural planes in enhancing

stress wave propagation. Conversely, when the stiffness falls below 2.8×10^6 Pa, y-direction permanent displacement, acceleration, and stress values remain largely unchanged as stiffness decreases. This aligns with real-world observations and highlights the critical role of stiffness thresholds in stress wave propagation.



2.2 Number of structural surfaces

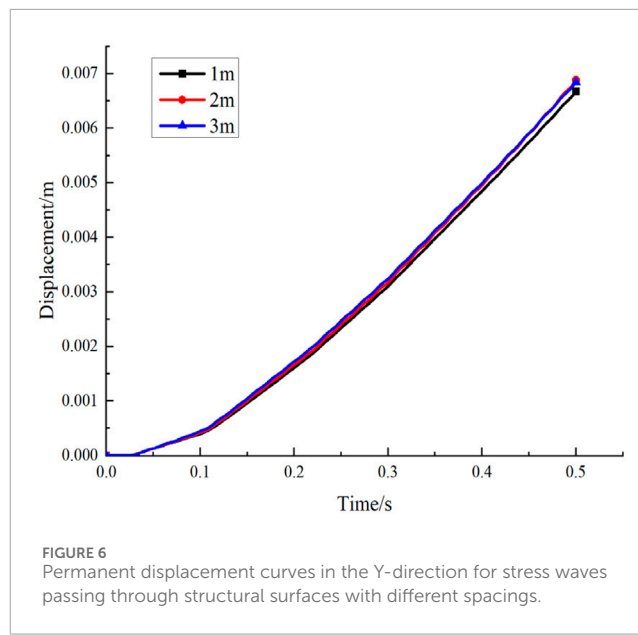
By varying the number of structural planes in a one-dimensional rock bar, the propagation behavior of stress waves through different quantities of structural planes is analyzed. As the number of structural planes increases, the spacing between them is kept at 1 m from the centerline.

We will discuss the scenarios of setting up single, two, three and four Zero-Thickness Structural Surface, respectively.

As shown in [Figure 5](#), with a single structural plane, the vertical permanent displacement exhibits the fastest rise and highest peak value. With two structural planes, positioned symmetrically outward from the center of the rock bar, the stress wave encounters the first plane earlier compared to the single-plane scenario. The stress wave undergoes attenuation from refraction and reflection as it passes through the first structural plane and propagates to the second. With three structural planes, attenuation intensifies compared to two; with four planes, propagation slows further, continuing this trend with additional planes. This demonstrates that increasing the number of structural planes amplifies refraction and reflection, resulting in continuous attenuation of the stress wave. As a result, the permanent displacement at the endpoint decreases progressively.

As shown the y-direction acceleration curves indicate that with an even number of structural planes, acceleration is detected earlier on the time axis, particularly at the spectral peak. For an odd number of structural planes, the spectral peak appears later in time. As the number of structural planes increases, the spectral peak shifts further in time, and the average acceleration value decreases progressively. This behavior correlates with the refraction and reflection phenomena, where more structural planes result in greater attenuation of the stress waves.

As shown the y-direction stress curves for stress waves passing through varying numbers of structural planes. The stress curve spectrum is detected earliest with four structural planes, followed



by three, two, and finally one. This indicates that fewer structural planes result in a slower arrival of the stress wave at the opposite endpoint. This phenomenon is attributed to the higher stiffness and elastic modulus of structural planes compared to the rock bar, along with energy dissipation during wave transmission. As noted in [Section 1.1](#), weaker structural planes induce significant refraction and reflection, reducing the stress wave's propagation speed. Increasing the number of structural planes is akin to raising the elastic modulus, aligning with observed results.

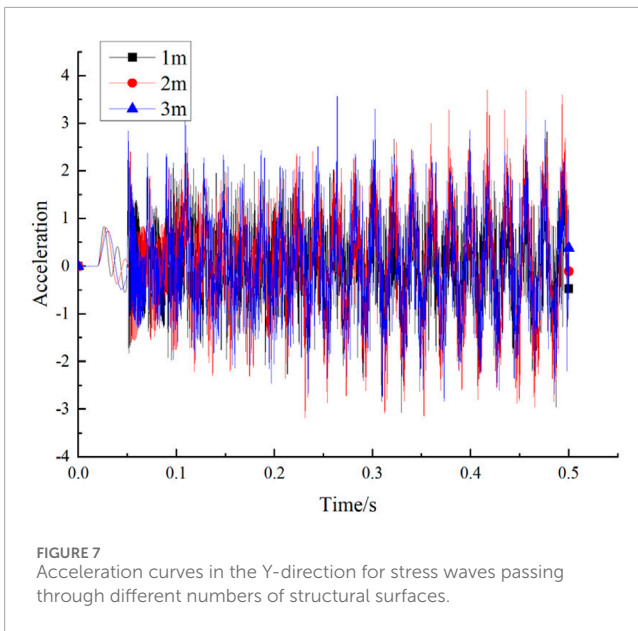
2.3 Variation in structural surface spacing

By adjusting the spacing of structural planes in a one-dimensional rock bar, we analyze the propagation behavior of stress waves through structural planes with varying spacings. Using the centerline as a reference, structural plane spacings of 1 m, 2 m, and 3 m are configured for analysis.

Using the midpoint of the rock mass as the baseline, structural plane spacings of 1 m, 2 m, and 3 m are chosen above and below to examine the impact of spacing on stress wave propagation. [Figure 6](#) shows that as structural plane spacing increases, the y-direction permanent displacement at the far end of the Hopkinson bar gradually rises, though the increase remains modest. This occurs because increasing the spacing between structural planes weakens refraction and reflection, resulting in higher permanent displacement. At larger structural plane spacings, reflections between planes nearly vanish, aligning with observed conditions.

[Figure 7](#) illustrates that as structural plane spacing increases, the y-direction acceleration at the far end of the Hopkinson bar gradually rises, though the increase remains modest. This is attributed to the reduced refraction and reflection between structural planes as their spacing increases, similar to the explanation for permanent displacement.

As shown the y-direction stress curves for stress waves passing through structural planes with varying spacings. When the



structural plane spacing is 1 m, the stress wave reaches the endpoint the earliest. With increasing structural plane spacing, the stress wave arrives at the endpoint progressively later. This occurs because wider structural plane spacing slows stress wave propagation and dissipates energy, resulting in a gradual reduction in the spectral peak value.

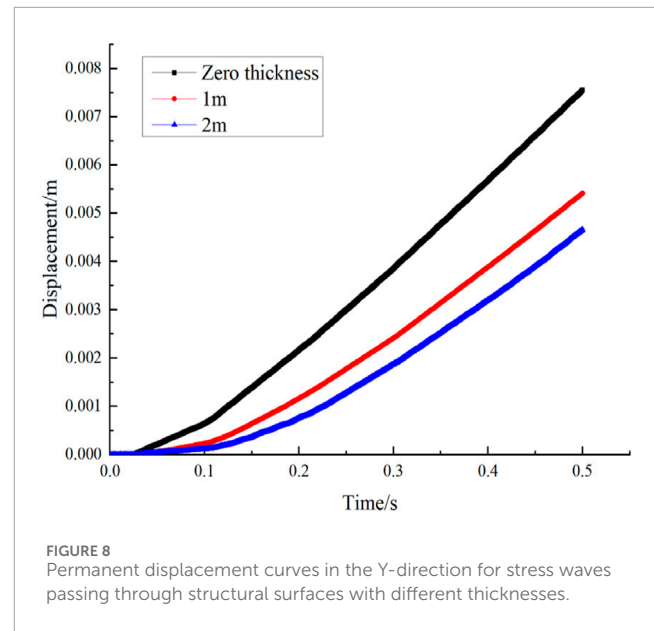
2.4 Variation in structural surface thickness

By adjusting the thickness of structural planes in a one-dimensional rock bar, we analyze the propagation behavior of stress waves through planes of varying thicknesses. Using the centerline as the reference, structural plane thicknesses of 0 m, 1 m, and 2 m are configured for analysis.

Using the midpoint of the rock mass as the baseline, structural planes with thicknesses of 0 m, 1 m, and 2 m are positioned above and below to examine the effect of thickness on stress wave propagation. Figure 8 shows that as the structural plane thickness increases from zero to 1 m and 2 m, the plane behaves as a weak interlayer, affecting stress wave propagation. As the thickness increases, the displacement and its growth rate over time gradually decrease. This aligns with field conditions, where weak interlayers absorb stress wave energy, enhancing refraction and reflection effects. Thicker weak interlayers amplify these effects, reducing permanent displacement, consistent with the numerical results.

As shown the y-direction acceleration is detected earliest when the structural plane has zero thickness. As the structural plane thickness increases, acceleration is detected later at the opposite end of the rock bar. Increasing structural plane thickness weakens stress wave propagation, affecting acceleration timing and magnitude, consistent with field observations.

As shown the y-direction stress curves, the spectral peak appears earliest for structural planes with zero thickness, while thicker planes delay the peak occurrence. Stress values are detected earliest at the opposite end of the rock bar when the structural plane has zero thickness. As structural plane thickness increases, point B detects



stress values at progressively later times. The maximum stress peak decreases as structural plane thickness increases, indicating that thicker planes weaken the stress wave propagation.

The above discussion reveals that greater structural plane thickness enhances its role as a weak interlayer, significantly attenuating stress wave values, consistent with observed conditions.

3 Influence of sawtooth-shaped structural surfaces

To study stress wave propagation through sawtooth-shaped structural planes, a sawtooth-shaped plane was positioned at the model's midpoint. The sawtooth angle was fixed at 60°, and the structural plane stiffness was varied at 2.8×10^6 Pa, 2.8×10^7 Pa, and 2.8×10^8 Pa. A sinusoidal velocity pulse (10 Hz, 1 m/s amplitude) was applied at the bottom surface, with fixed constraints and viscoelastic boundary conditions at the base. Permanent displacement, acceleration, and stress were monitored at the opposite midpoint to examine the influence of structural plane stiffness on stress wave propagation. Subsequently, sawtooth angles of 30°, 60°, 90°, 120°, 150°, and 180° were tested to analyze their effects on stress wave propagation. The model dimensions were 100 m × 1 m, with a triangular mesh, as depicted in Figure 9.

3.1 Stiffness of Sawtooth-Shaped structural surfaces

We will discuss the scenarios where Stiffness values is set to stiffness values of 2.8×10^6 Pa, 2.8×10^7 Pa and 2.8×10^8 Pa, respectively.

Varying the stiffness of the 60° sawtooth-shaped structural plane yielded vertical permanent displacement curves for different stiffness values, as shown in Figure 10 at a stiffness of 2.8×10^6 Pa, the sawtooth-shaped structural plane exhibited negligible permanent

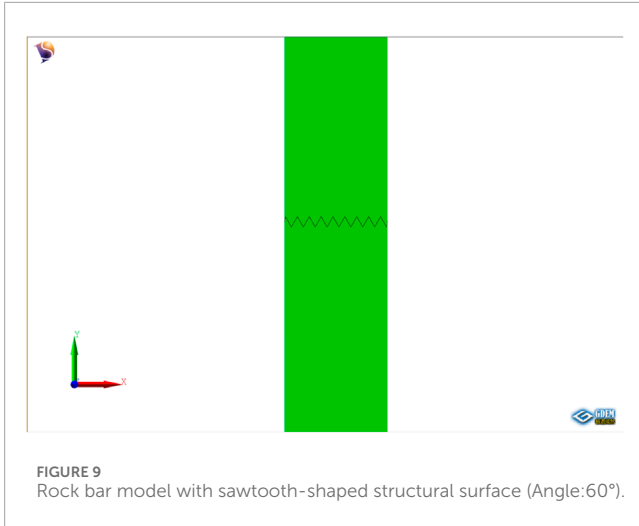


FIGURE 9 Rock bar model with sawtooth-shaped structural surface (Angle:60°).

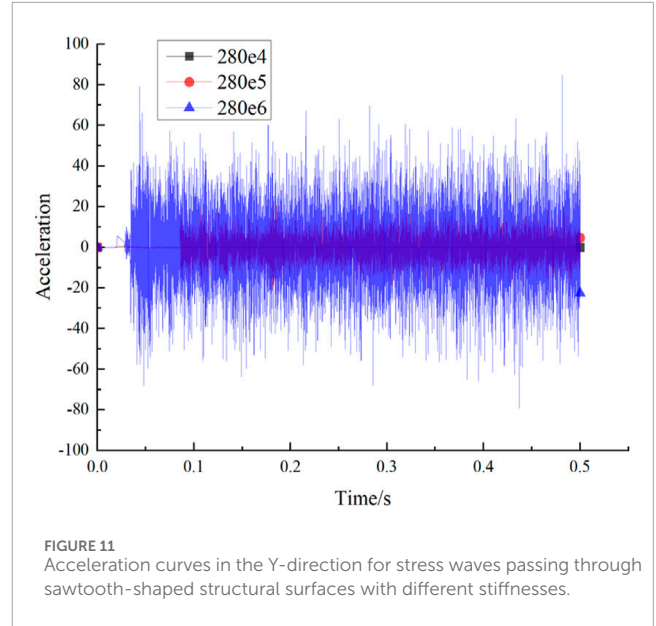


FIGURE 11 Acceleration curves in the Y-direction for stress waves passing through sawtooth-shaped structural surfaces with different stiffnesses.

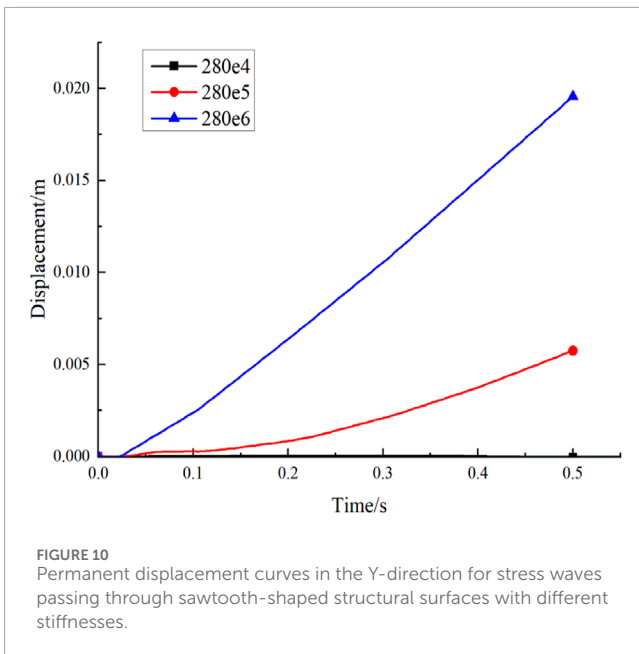


FIGURE 10 Permanent displacement curves in the Y-direction for stress waves passing through sawtooth-shaped structural surfaces with different stiffnesses.

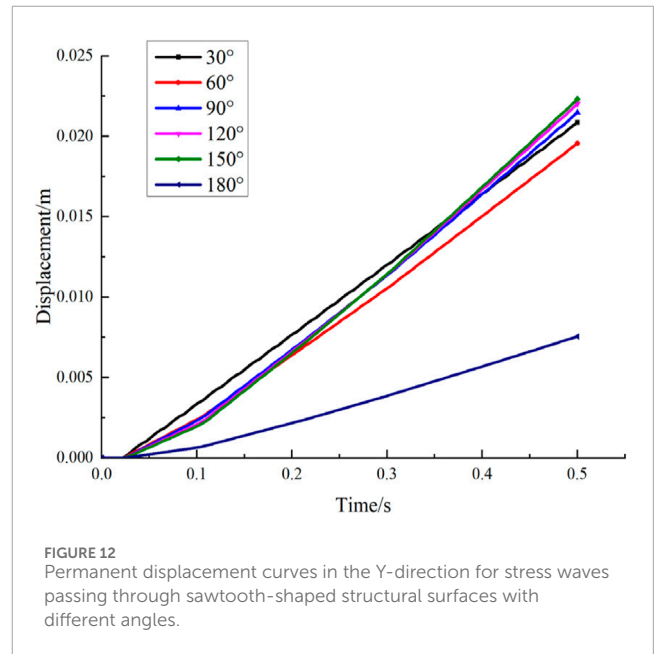


FIGURE 12 Permanent displacement curves in the Y-direction for stress waves passing through sawtooth-shaped structural surfaces with different angles.

displacement. As the stiffness of the sawtooth-shaped structural plane increased, permanent displacement rose accordingly, indicating a positive correlation.

This observation aligns with real-world conditions: low structural plane stiffness behaves similarly to the rock bar material, exerting minimal influence on permanent displacement. Noticeable permanent displacement occurs only when the stiffness of the sawtooth-shaped structural plane equals or exceeds that of the rock bar.

Figure 11 shows that the y-direction acceleration curves of stress waves propagating through sawtooth-shaped structural planes exhibit significantly lower stress and acceleration values when the stiffness is below the normal level (2.8×10^6 Pa), with notable differences observed. This confirms that high-stiffness sawtooth planes enhance stress wave transmission, whereas low stiffness increases wave attenuation and energy dissipation.

3.2 Sawtooth-Shaped Structural surface inclination

We will discuss the scenarios where the angle of the sawtooth structural surface is set to 30°, 60°, 90°, 120°, 150°, and 180°, respectively.

Figure 12 shows that the permanent displacement after stress wave propagation is smallest for a sawtooth-shaped structural plane with a 180° angle (horizontal), indicating that sawtooth structures significantly affect displacement. At a 30° sawtooth angle, the displacement exhibits the highest initial growth rate and peak value. For other angles, displacement growth rates are similar initially but diverge after 0.2 s. The descending order of permanent displacement is $150^\circ > 120^\circ > 90^\circ > 30^\circ > 60^\circ > 180^\circ$.

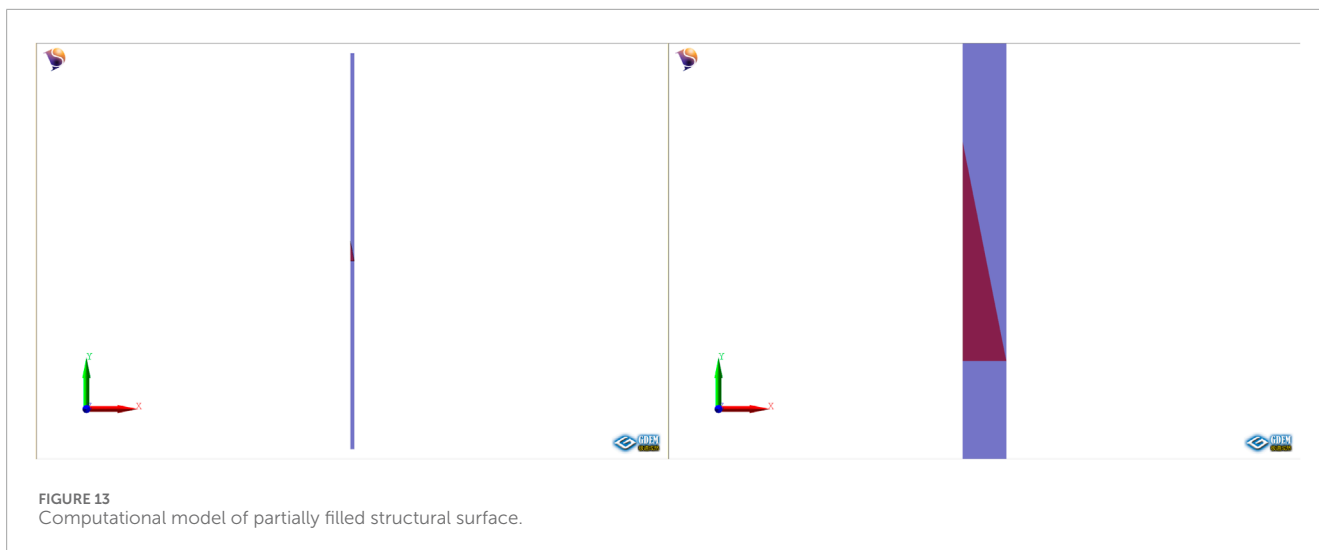


FIGURE 13 Computational model of partially filled structural surface.

TABLE 2 Material parameters of the rock bar model and filling material.

Rock bar model parameter	Density (kg/m ³)	Elastic modulus (Pa)	Poisson's ratio	Cohesion (Pa)	Tensile strength (Pa)	Friction angle (°)
	2700	6.5628e10	0.2	4.0e5	2.0e5	35
Filling Material Parameter	Density (kg/m ³)	Elastic Modulus (Pa)	Poisson's Ratio	Cohesion (Pa)	Tensile Strength (Pa)	Friction Angle (°)
	1800	1.0e8	0.15	1.0e5	1.5e5	15

As shown the y-direction acceleration curves exhibit varying spectral peak values depending on the sawtooth-shaped structural plane angle. The smallest peak value occurs at 180°. As the sawtooth angle increases, stress and acceleration values decrease, following the order 180° < 150° < 120° < 90° < 60° < 30°. This trend aligns with actual observations, as larger angles enhance refraction, reflection, and attenuation effects.

4 Influence of filled structural surfaces

As illustrated in Figure 13, a 1 m × 5 m filled structural plane was positioned at the midpoint of the one-dimensional rock bar to examine how varying filling degrees and materials affect stress wave propagation.

4.1 Fully filled and partially filled structural surfaces

The material parameters of the rock bar model and the filling material are shown in Table 2.

As illustrated in Figure 14, a structural plane with a 5 m thickness was subjected to two filling conditions: full filling and half filling, the latter involving a diagonal triangular fill, to analyze the

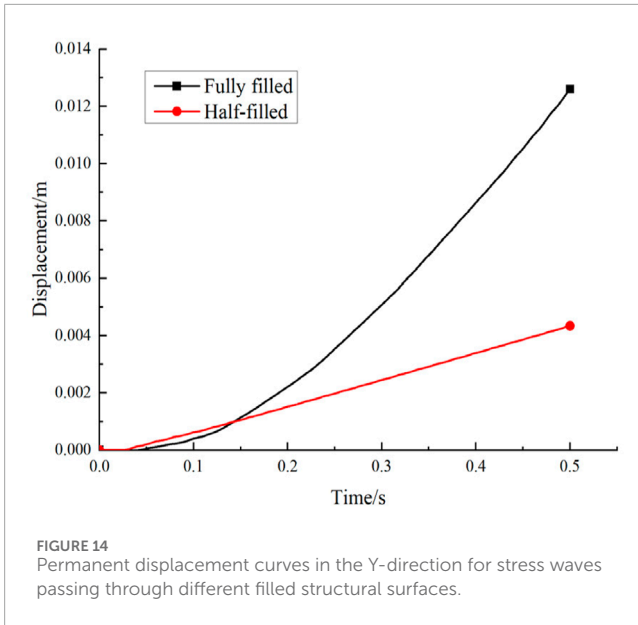
y-direction acceleration curves of stress waves. During the initial 0–0.15 s, the triangular filling method enabled the half-filled case to transmit the stress wave more quickly. As a result, within this interval, the half-filled case exhibited greater displacement and growth rates compared to the fully filled case. After 0.15 s, as the stress wave finishes propagating through the filled region, the fully filled case exhibits a rapid increase in speed, ultimately resulting in a final displacement approximately 300% greater than that of the half-filled case.

As shown the y-direction acceleration curves reveal that at the initial moment, stress and acceleration values are first detected in the half-filled structural plane. Over time, the stress and acceleration values at the opposite end of the rock bar for both fully filled and half-filled structural planes tend to converge, showing upward and downward waveform fluctuations.

Figure 14 and the y-direction acceleration curves demonstrate that fully filled structural planes attenuate stress wave propagation energy more effectively than partially filled or unfilled ones, likely due to the absorption and scattering effects of the filling materials.

4.2 Influence of different filling materials

By altering the density of the filling materials, we analyzed the propagation behavior of stress waves through materials with varying



densities. Table 3 provides the material parameters of the rock bar model and the various filling materials used in the simulations.

As shown in Figure 15, structural planes were filled with materials of varying densities. The permanent displacement at the opposite end of the rock bar increases with higher filling densities. The permanent displacement at 2,000 kg/m³ is notably higher than at 1,800 kg/m³ and 1,700 kg/m³, attributed to the reduced influence of the weak interlayer.

The stress and acceleration curves reveal that waveform values appear earliest for a density of 2,000 kg/m³, followed by 1,800 kg/m³, and lastly for the lowest density. This demonstrates that higher density results in faster stress wave propagation.

Figures 15, 16 show that increasing the density of the filling material enhances the propagation speed of stress waves and reduces energy attenuation, leading to higher permanent displacement and acceleration values. This suggests that high-density filling materials improve stress wave propagation efficiency and minimize energy loss.

5 Influence of wave impedance on stress wave propagation

To study the propagation of stress waves influenced by wave impedance, a zero-thickness structural plane was placed at the model's midpoint, with loess material above and rock material below. A 10 Hz sinusoidal velocity pulse with a 1 m/s amplitude was applied at the bottom surface under fixed constraints. Monitoring at the upper surface midpoint was used to examine stress wave propagation under different loess densities and damping ratios. Material parameters for the loess are listed in Table 4, and the computational model for wave-impedance filling is illustrated in Figure 17.

We will discuss the scenarios where loess is set to normal density, density reduced by 10 times, and density increased by 10 times, respectively.

As shown in Figure 18, the y-direction acceleration curves for stress waves passing through a wave-impedance structural plane demonstrate that increasing or decreasing the density of loess by a factor of ten, relative to the normal density, results in an inverse relationship between density and displacement, with higher densities corresponding to smaller displacements.

As illustrated in Figure 19, the density increases, the peak acceleration value decreases, demonstrating a negative correlation. When a significant wave impedance mismatch exists between the materials above and below the structural plane, both the amplitude and propagation speed of the stress wave are notably reduced, highlighting the critical role of wave impedance matching in stress wave propagation.

6 Influence of damping on stress wave propagation

6.1 Definition and impact of damping

In static problems, adjusting the damping coefficient ensures convergence to a static state, with convergence speed directly proportional to the damping magnitude. Insufficient damping causes repeated oscillation of mesh nodes (Gagnon et al., 2019). In dynamic analyses, damping represents the energy dissipation in elastoplastic materials, such as rock and soil, during deformation and failure. Damping significantly affects wave propagation and the dynamic response of geotechnical structures. Excessive or insufficient damping can lead to divergent results, failing to represent actual conditions. Thus, selecting an appropriate damping coefficient is essential for ensuring accurate calculation results.

The governing equation for the motion of grid nodes is given by Equation 1:

$$m\ddot{u}_i + c\dot{u}_i + F_i e = F \tag{1}$$

For the characteristic time, assume $T_e = 2\pi\sqrt{m/K}$, $t = T_e t'$, the governing equation becomes Equation 2:

$$\ddot{u}_i + \frac{2\pi c}{\sqrt{mK}}\dot{u}_i + \frac{4\pi^2}{K}F_i e = \frac{4\pi^2}{K}F \tag{2}$$

ζ represents the dimensionless damping ratio. Its expression is given by Equation 3:

$$\zeta = \frac{2\pi c}{\sqrt{mK}} \tag{3}$$

From Equation 3, we can obtain the expression for c , which is Equation 4, consequently,

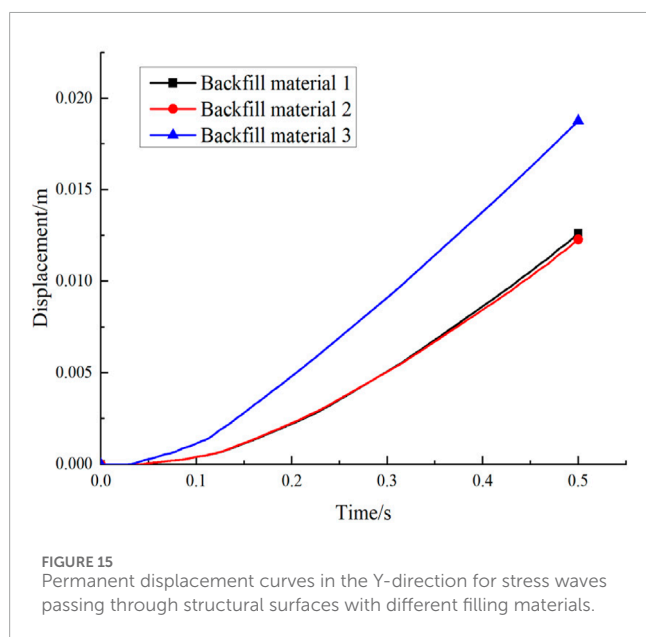
$$c = \frac{1}{2\pi}\zeta\sqrt{mK} \tag{4}$$

In the formula, m represents mass, c represents damping, K represents element stiffness, F represents force, $F_i e$ represents nodal force, T_e represents characteristic time, \ddot{u}_i represents acceleration, \dot{u}_i represents velocity.

The damping ratio influences the natural frequency and vibration duration of elastoplastic materials such as rock and soil.

TABLE 3 Material parameters of rock bar model and different filling materials.

	Density (kg/m ³)	Elastic modulus (Pa)	Poisson's ratio	Cohesion (Pa)	Tensile strength (Pa)	Friction angle (°)
Rock Bar Material	2700	65.628e9	0.2	4.0e5	2.0e5	35
Filling Material 1	1700	1.0e8	0.15	1.0e5	1.5e5	15
Filling Material 2	1800	1.0e8	0.15	1.0e5	1.5e5	15
Filling Material 3	2000	1.0e8	0.15	1.0e5	1.5e5	15



In dynamic calculations, adjusting the damping ratio modifies vibration duration, allowing the system's damping ratio to be inversely determined from shaking table experiment results.

6.2 Effect of different damping levels

We will discuss the scenarios where the damping is set to 0, 0.4, and 0.8, respectively.

As illustrated in Figure 20, by varying damping values to study the stress wave propagation process, displacement curves reveal that higher damping increases energy dissipation, leading to smaller endpoint displacements.

As illustrated in Figure 21, the axial stress and acceleration curves reveal that as the damping ratio increases, stress loss intensifies, resulting in progressively smaller stress and acceleration values. Higher damping ratios accelerate energy dissipation, significantly reducing the stress wave amplitude at the propagation endpoint. This highlights the crucial role of damping in wave energy attenuation, particularly in complex geological conditions where damping effects can critically influence slope stability.

7 Conclusion

7.1 Formation mechanism

The propagation characteristics of stress waves in rock slopes are governed by various factors, including the characteristics and parameters of structural planes, wave impedance, and damping. These elements collectively contribute to attenuation of stress wave amplitude, signal delay, and reduced wave speed, the physical mechanism is primarily manifested in the following two aspects. Firstly, the complexity of structural planes: in actual rock masses, the characteristics of structural planes are extremely complex, including varying dip angles, fill materials, stiffness, density, undulations, etc. These factors directly affect the reflection, refraction, and transmission of stress waves at the structural planes. For example, at inclined structural planes, stress waves may undergo refraction and reflection, leading to tensile cracking and slippage at the planes; the fill materials within the structural planes may absorb part of the wave energy, reducing the amplitude of the wave after it passes through; fill materials of different shapes can cause both refraction and reflection in addition to reducing the wave amplitude, resulting in more complex mechanical behaviors. Secondly, the

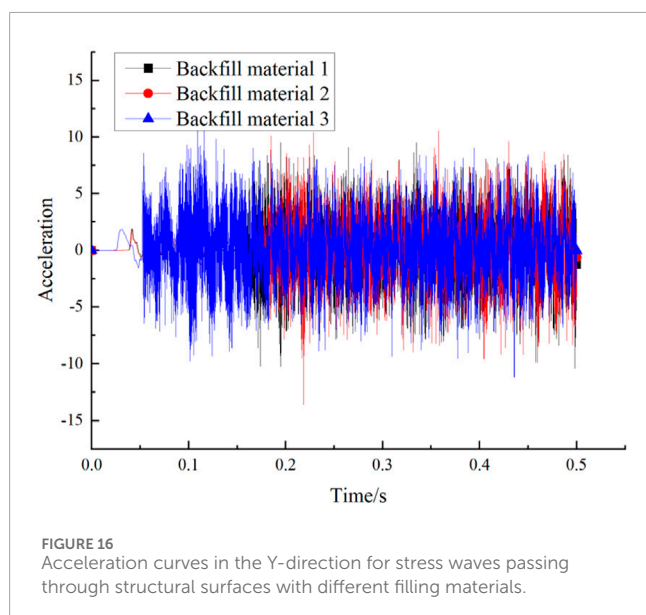
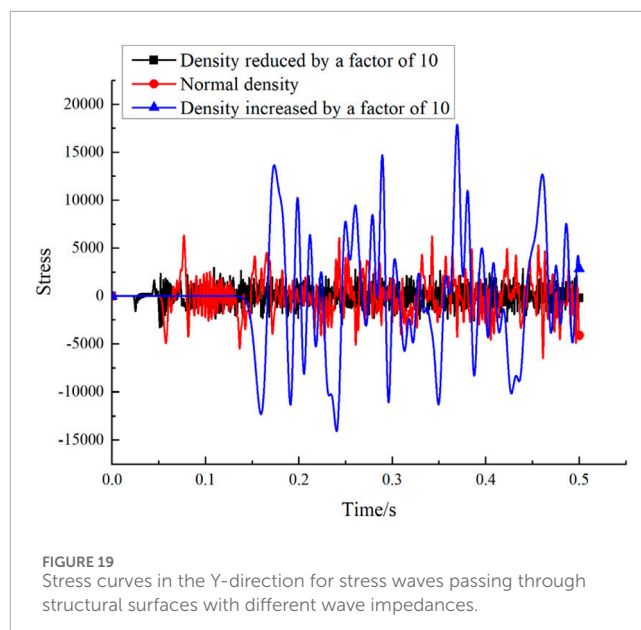
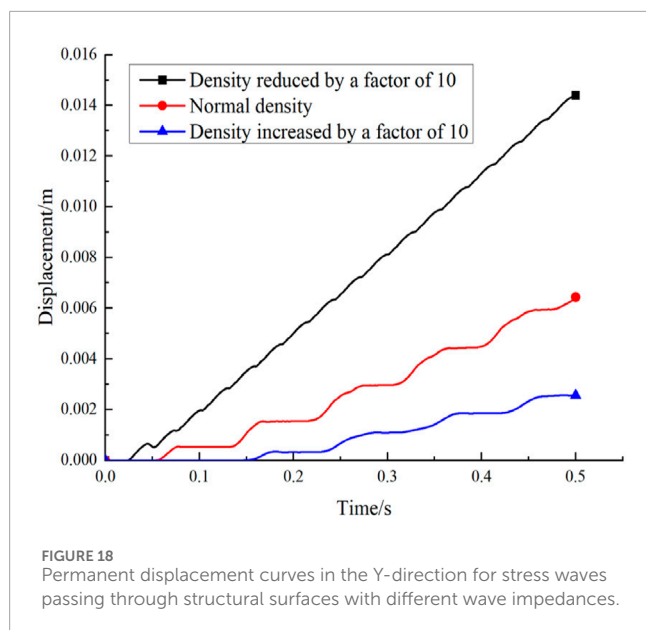
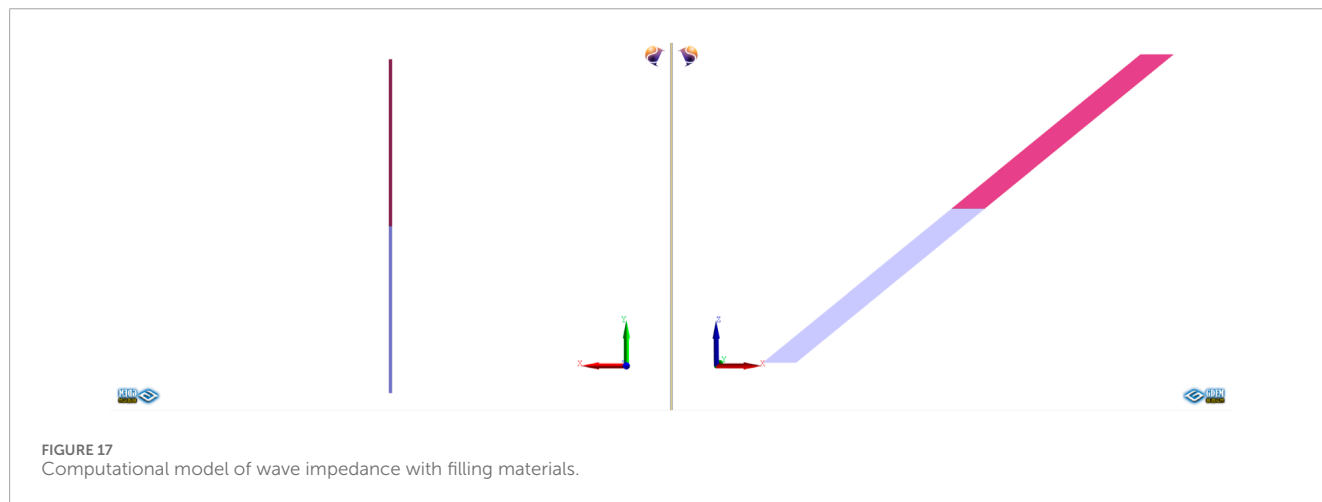


TABLE 4 Material parameters of rock bar model and loess material.

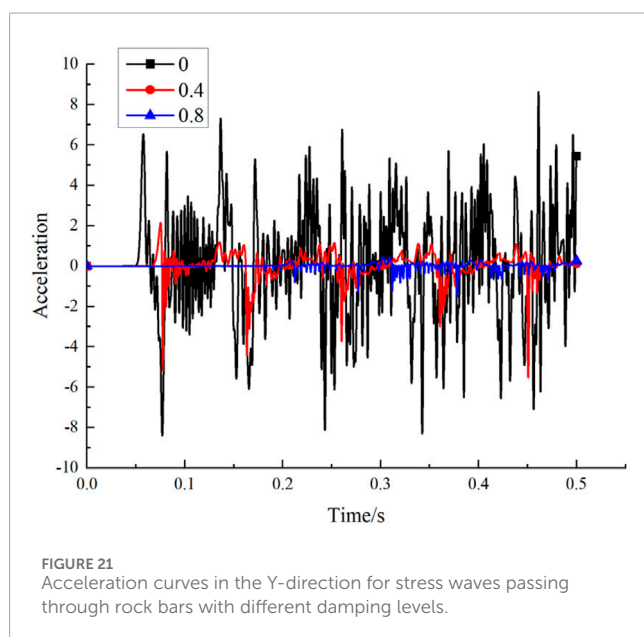
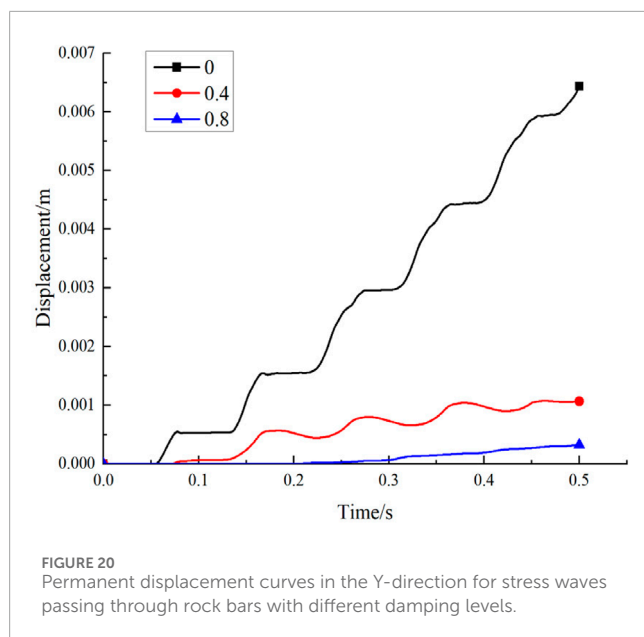
	Density (kg/m ³)	Elastic modulus (Pa)	Poisson's ratio	Cohesion (Pa)	Tensile strength (Pa)	Friction angle (°)
Rock Bar Material	2700	6.5628e10	0.2	4.0e5	2.0e5	35
Loess Material	1500	1.748e9	0.27	1.05e5	2.0e5	22.8



interaction between waves and structural planes: when stress waves propagate to a structural plane, part of the wave is reflected back into the original medium, while another part is transmitted into the adjacent medium. This interaction depends on the properties of the wave (such as frequency, wavelength) and the characteristics of the structural plane (such as roughness, continuity). If the structural plane is rough, the wave will undergo multiple scattering during propagation, leading to dispersion and attenuation of wave energy.

7.2 Conclusion

Using a one-dimensional Hopkinson bar model, this study systematically analyzed stress wave propagation under various structural plane conditions, monitoring key parameters such as permanent displacement, acceleration, and stress values. The following well-structured conclusions were drawn:



7.2.1 The critical influence of structural plane characteristics on stress wave propagation

- Structural plane stiffness is a critical factor in controlling stress wave propagation efficiency. When stiffness exceeds a critical threshold (2.8×10^6 Pa), permanent displacement, acceleration, and stress values increase significantly, emphasizing the role of high-stiffness structural planes in enhancing wave propagation. Below this threshold, these parameters exhibit minimal variation, underscoring the stiffness threshold's importance in the propagation process.
- Structural plane characteristics significantly affect stress wave propagation. Increasing the number of structural planes enhances wave refraction and reflection, leading

to gradual attenuation. Conversely, increasing the spacing between structural planes improves propagation, resulting in higher permanent displacement, acceleration, and stress values. However, increased structural plane thickness mimics a weak interlayer, hindering wave propagation and reducing these parameters.

7.2.2 Unique effects of Sawtooth-Shaped structural planes

- The angle and stiffness of sawtooth-shaped structural planes jointly influence the propagation path and energy distribution of stress waves. As the angle increases (from 30° to 180°), stress wave refraction and reflection gradually intensify, significantly reducing the peak values of permanent displacement and acceleration. This highlights the critical role of the sawtooth-shaped structural plane angle in stress wave energy dissipation.
- Variations in the stiffness of sawtooth-shaped structural planes also significantly impact wave propagation efficiency. High-stiffness sawtooth planes transmit stress waves more effectively, whereas low stiffness causes wave attenuation and energy dissipation, underscoring the crucial role of stiffness in propagation.

7.2.3 Influence of filling materials

- The filling form of structural planes and the density of filling materials significantly influence stress wave propagation. Fully filled structural planes attenuate stress wave propagation energy more effectively than partially filled or unfilled planes. This is likely due to the absorption and scattering effects of filling materials on stress waves.
- Higher filling material density increases stress wave propagation speed and reduces energy attenuation. This leads to higher permanent displacement and acceleration, indicating that high-density filling materials enhance stress wave propagation efficiency and minimize energy loss.

7.2.4 Effects of wave impedance matching and damping

- Differences in wave impedance critically affect stress wave propagation characteristics across structural planes. When wave impedance differs significantly across the structural plane, stress wave amplitude and propagation speed decrease significantly. This underscores the critical role of wave impedance matching in stress wave propagation.
- Increasing the damping ratio enhances energy dissipation, significantly reducing the stress wave amplitude at the propagation endpoint. This highlights the crucial role of damping in wave energy attenuation, particularly under complex geological conditions, where damping can significantly influence slope stability.

However, the intrinsic complexity of structural planes in actual rock masses, including dip angles, fillers, stiffness, and density, among other characteristics, still remains difficult to fully

simulate. Most studies discussed in this paper focus on either single characteristics or simple combinations of structural planes, thus failing to fully capture the complexity of structural planes in natural rock masses. Furthermore, the interaction between stress wave propagation and multi-field coupling effects (such as ground stress and groundwater) has yet to be investigated. Future research efforts should be dedicated to more accurately simulating the complexity of structural planes, conducting in-depth analyses of multi-physical field coupling effects, improving the reliability of experimental data, and verifying as well as enhancing the practicality of theoretical models. These efforts will provide a more comprehensive understanding of how structural plane characteristics influence stress wave propagation patterns.

In summary, this study employed a one-dimensional Hopkinson bar model to simulate stress wave propagation under varying structural plane conditions, systematically analyzing the effects of structural plane characteristics, sawtooth-shaped features, filling materials, wave impedance, and damping on stress wave propagation. Despite certain limitations in the research process, the results achieved undoubtedly lay a solid foundation for future explorations in this field. These findings offer a solid theoretical foundation for analyzing rock mass dynamics and slope stability, while also providing valuable guidance for engineering design and disaster prevention in complex geological settings.

Data availability statement

The raw data supporting the conclusions of this article will be made available by the authors, without undue reservation.

Author contributions

PJ: Writing—original draft, Writing—review and editing. WZ: Writing—review and editing. HW: Software, Writing—original draft. YW: Formal Analysis, Writing—original draft. HY: Writing—review and editing.

References

- Aligholi, S., and Khandelwal, M. (2022). Computing elastic moduli of igneous rocks using modal composition and effective medium theory. *Geosciences* 12 (11), 413. doi:10.3390/geosciences12110413
- Chai, S., Tian, W., Yu, L., and Wang, H. (2020). Numerical study of ground vibrations caused by cylindrical wave propagation in a rock mass with a structural plane. *Shock Vib.* 2020 (1), 1–9. doi:10.1155/2020/4681932
- Chen, F., Zong, Z., and Yin, X. (2022). Acoustoelastometry for joint effects of stress and thermal fields on wave dispersion and attenuation. *J. Geophys. Res. Solid Earth* 127 (4), e2021JB023671. doi:10.1029/2021jb023671
- Chong, S.-H., Kim, J.-W., Cho, G.-C., and Song, K.-I. (2020). Preliminary numerical study on long-wavelength wave propagation in a jointed rock mass. *Geomech. Eng.* 21 (3), 227–236. doi:10.12989/gae.2020.21.3.227
- Fan, L., Ma, G., and Li, J. (2012). Nonlinear viscoelastic medium equivalence for stress wave propagation in a jointed rock mass. *Int. J. Rock Mech. Min. Sci.* 50, 11–18. doi:10.1016/j.ijrmms.2011.12.008
- Fan, L., Wang, M., and Wu, Z. (2021). Effect of nonlinear deformational macrojoint on stress wave propagation through a double-scale discontinuous rock mass. *Rock Mech. Rock Eng.* 54, 1077–1090. doi:10.1007/s00603-020-02308-8
- Fan, Z., and Cai, J. (2021). Effects of unidirectional *in situ* stress on crack propagation of a jointed rock mass subjected to stress wave. *Shock Vib.* 2021 (1), 5529540. doi:10.1155/2021/5529540
- Feng, X., Zhang, Q., Wang, E., Ali, M., Dong, Z., and Zhang, G. (2020). 3D modeling of the influence of a splay fault on controlling the propagation of nonlinear stress waves induced by blast loading. *Soil Dyn. Earthq. Eng.* 138, 106335. doi:10.1016/j.soildyn.2020.106335
- Gagnon, L., Morandini, M., and Ghiringhelli, G. L. (2019). A review of particle damping modeling and testing. *J. Sound Vib.* 459, 114865. doi:10.1016/j.jsv.2019.114865
- Guo, Y., Ying, Q., Wang, D., Zhang, H., Huang, F., Guo, H., et al. (2022). Experimental study on shear characteristics of structural plane with different fluctuation characteristics. *Energies* 15 (20), 7563. doi:10.3390/en15207563
- Hong, S., Li, H., and Rong, L. (2021). Experimental study on stress wave propagation crossing the jointed specimen with different JRCs. *Shock Vib.* 2021 (1), 3096253. doi:10.1155/2021/3096253
- Huang, J., Liu, X., Zhao, J., Wang, E., and Wang, S. (2020a). Propagation of stress waves through fully saturated rock joint under undrained conditions and dynamic response characteristics of filling liquid. *Rock Mech. Rock Eng.* 53, 3637–3655. doi:10.1007/s00603-020-02126-y
- Huang, X., Qi, S., Zheng, B., Liu, Y., Xue, L., and Liang, N. (2020b). Stress wave propagation through rock joints filled with viscoelastic medium considering different water contents. *Appl. Sci.* 10 (14), 4797. doi:10.3390/app10144797

Funding

The author(s) declare that no financial support was received for the research, authorship, and/or publication of this article.

Conflict of interest

The authors declare that the research was conducted in the absence of any commercial or financial relationships that could be construed as a potential conflict of interest.

Generative AI statement

The author(s) declare that no Generative AI was used in the creation of this manuscript.

Publisher's note

All claims expressed in this article are solely those of the authors and do not necessarily represent those of their affiliated organizations, or those of the publisher, the editors and the reviewers. Any product that may be evaluated in this article, or claim that may be made by its manufacturer, is not guaranteed or endorsed by the publisher.

Supplementary material

The Supplementary Material for this article can be found online at: <https://www.frontiersin.org/articles/10.3389/feart.2025.1534007/full#supplementary-material>

- Jia, S., Wang, Z., Wang, J., Lu, Z., and Wang, H. (2021). Experimental and theoretical study on the propagation characteristics of stress wave in filled jointed rock mass. *Plos one* 16 (9), e0253392. doi:10.1371/journal.pone.0253392
- Kim, J.-W., Chong, S.-H., and Cho, G.-C. (2021). Effects of gouge fill on elastic wave propagation in equivalent continuum jointed rock mass. *Materials* 14 (12), 3173. doi:10.3390/ma14123173
- Kononenko, M., and Khomenko, O. (2021). New theory for the rock mass destruction by blasting, in *Mining of mineral deposits*.
- Li, J., Li, H., Ma, G., and Zhao, J. (2012). A time-domain recursive method to analyse transient wave propagation across rock joints. *Geophys. J. Int.* 188 (2), 631–644. doi:10.1111/j.1365-246x.2011.05286.x
- Li, N., Zhou, Y., and Li, H. (2021). Experimental study for the effect of joint surface characteristics on stress wave propagation. *Geomechanics Geophys. Geo-Energy Geo-Resources* 7 (3), 50. doi:10.1007/s40948-021-00235-8
- Liu, E., Hudson, J. A., and Pointer, T. (2000). Equivalent medium representation of fractured rock. *J. Geophys. Res. Solid Earth* 105 (B2), 2981–3000. doi:10.1029/1999jb900306
- Liu, X., Liu, Q., He, J., and Yu, F. (2020). Numerical simulation of cracking process in rock mass under the coupled thermo-mechanical condition. *Int. J. Comput. Methods* 17 (09), 1950065. doi:10.1142/s0219876219500658
- Lou, X., Sun, M., and Yu, J. (2021). Stress wave propagation in different number of fissured rock mass based on nonlinear analysis. *Int. J. Nonlinear Sci. Numer. Simul.* 22 (7-8), 943–954. doi:10.1515/ijnsns-2019-0301
- Müller, T. M., Gurevich, B., and Lebedev, M. (2010). Seismic wave attenuation and dispersion resulting from wave-induced flow in porous rocks—a review. *Geophysics* 75 (5), 75A147–75A164. doi:10.1190/1.3463417
- Nolte, D., Pyrak-Nolte, L., Beachy, J., and Ziegler, C. (2000). Transition from the displacement discontinuity limit to the resonant scattering regime for fracture interface waves. *Int. J. Rock Mech. Min. Sci.* 37 (1-2), 219–230. doi:10.1016/s1365-1609(99)00102-1
- Qin, Z., Zhao, Y., Chen, L., Cao, H., Zeng, L., Jiao, W., et al. (2023). Propagation characteristics and control technology of blasting vibration in neighborhood tunnel. *Front. Earth Sci.* 11, 1204450. doi:10.3389/feart.2023.1204450
- Rong, H., Li, N., Cao, C., Wang, Y., Li, J., and Li, M. (2024). Numerical simulation of rock blasting under different *in-situ* stresses and joint conditions. *Plos one* 19 (4), e0299258. doi:10.1371/journal.pone.0299258
- Shafique, S., Afzal, M., and Nawaz, R. (2020). On the attenuation of fluid–structure coupled modes in a non-planar waveguide. *Math. Mech. Solids* 25 (10), 1831–1850. doi:10.1177/1081286520911443
- Song, D., Liu, X., Huang, J., Wang, E., and Zhang, J. J. B. (2021). Characteristics of wave propagation through rock mass slopes with weak structural planes and their impacts on the seismic response characteristics of slopes: a case study in the middle reaches of Jinsha River, *Bulletin of Engineering Geology and the Environment*, 80, 1317–1334.
- Song, L. (2012). *Research into the dynamic characteristics of stress wave propagation in jointed rock*. Shaanxi, China: Xi'an University of Architecture and Technology.
- Wang, J., Yin, Y., and Esmaili, K. (2018). Numerical simulations of rock blasting damage based on laboratory-scale experiments. *J. Geophys. Eng.* 15 (6), 2399–2417. doi:10.1088/1742-2140/aac117
- Wang, T., Li, P., Tang, C. a., Zhang, B., and Yu, J. (2023). Finite element analysis for the mechanism of stress wave propagation and crack extension due to blasting of a frozen rock mass. *Sustainability* 15 (5), 4616. doi:10.3390/su15054616
- Wang, Y., Tang, Y., Zhang, F., and Guo, J. (2022). Laboratory model tests of seismic strain response of anti-seismic anchor cables. *Front. Earth Sci.* 10, 863511. doi:10.3389/feart.2022.863511
- Wei, Z., Li, X., Cao, H., and Wu, T. (2024). Frequency distribution of different joint slopes containing ceramic soil under seismic wave action. *Front. Earth Sci.* 12, 1429551. doi:10.3389/feart.2024.1429551
- White, J. E. (2000). *Underground sound: application of seismic waves*.
- Xia, Y., Zhang, C., Zhou, H., Chen, J., Gao, Y., Liu, N., et al. (2020). Structural characteristics of columnar jointed basalt in drainage tunnel of Baihetan hydropower station and its influence on the behavior of P-wave anisotropy. *Eng. Geol.* 264, 105304. doi:10.1016/j.enggeo.2019.105304
- Xiroudakis, G., Saratsis, G., and Lazos, I. (2023). Implementation of the displacement discontinuity method in geotechnical case studies. *Geosciences* 13 (9), 272. doi:10.3390/geosciences13090272
- Yu, J., Song, B., and Qian, Q. (2012). Study of propagation of P-waves in dual nonlinear elastic rock medium with one set of joints. *Chin. J. Rock Mech. Eng.* 31 (12), 2400–2411. doi:10.3969/j.issn.1000-6915.2012.12.003
- Yu, J., Zhang, Z., Wu, G., Li, X., and Tian, H. (2024). Investigation on asymmetric dynamic response characteristics of anchored surrounding rock under blasting excavation of inclined layered rock tunnel. *Can. Geotechnical J. (ja)*. doi:10.1139/cgj-2024-0250
- Zarastvand, M., Ghassabi, M., and Talebitooti, R. (2022). Prediction of acoustic wave transmission features of the multilayered plate constructions: a review. *J. Sandw. Struct. Mater.* 24 (1), 218–293. doi:10.1177/1099636221993891
- Zeng, S., Wang, S., Sun, B., and Liu, Q. (2018). Propagation characteristics of blasting stress waves in layered and jointed rock caverns. *Geotech. Geol. Eng.* 36, 1559–1573. doi:10.1007/s10706-017-0410-x
- Zhang, Y., Zhu, J., Xu, H., Han, D., and Bao, W. (2024). Examining theoretical applicability of displacement discontinuity model to wave propagation across rock discontinuities. *J. Rock Mech. Geotechnical Eng.* doi:10.1016/j.jrmge.2024.06.006
- Zheng, H., Sladek, J., Sladek, V., Wang, S., and Wen, P. (2021). Hybrid meshless/displacement discontinuity method for FGM Reissner's plate with cracks. *Appl. Math. Model.* 90, 1226–1244. doi:10.1016/j.apm.2020.10.023
- Zheng, W., Cao, Y., Fan, W., Liang, X., Yuan, S., Gao, W., et al. (2024). Formation processes and mechanisms of a fault-controlled colluvial landslide in the Qinling-Daba Mountains, China. *Sci. Rep.* 14 (1), 19167. doi:10.1038/s41598-024-69835-0
- Zhou, L., Zheng, Y., Ma, H., and Song, G. (2021). Attenuation characteristics of stress wave in cracked concrete beam using smart aggregate transducers enabled time-reversal technique. *J. Intelligent Material Syst. Struct.* 32 (4), 473–485. doi:10.1177/1045389x20953619
- Zhu, J., Ren, M., and Liao, Z. (2020). Wave propagation and diffraction through non-persistent rock joints: an analytical and numerical study. *Int. J. Rock Mech. Min. Sci.* 132, 104362. doi:10.1016/j.ijrmm.2020.104362